IEEE Access
Multidisciplinary | Rapid Review | Open Access Journal

Received August 8, 2019, accepted August 31, 2019, date of publication September 9, 2019, date of current version September 20, 2019.

Digital Object Identifier 10.1109/ACCESS.2019.2940114

Driving Intention Identification Based on Long Short-Term Memory and A Case Study in Shifting Strategy Optimization

YONGGANG LIU[1,2], (Senior Member, IEEE), PAN ZHAO[1,2], DATONG QIN[1,2], GUANG LI[3], (Member, IEEE), ZHENG CHEN[4], (Senior Member, IEEE), AND YI ZHANG[5]

[1]State Key Laboratory of Mechanical Transmissions, Chongqing University, Chongqing 400044, China
[2]School of Automotive Engineering, Chongqing University, Chongqing 400044, China
[3]School of Engineering and Materials Science, Queen Mary University of London, London E1 4NS, U.K.
[4]Faculty of Transportation Engineering, Kunming University of Science and Technology, Kunming 650500, China
[5]Department of Mechanical Engineering, University of Michigan–Dearborn, Dearborn, MI 48128, USA

Corresponding authors: Yonggang Liu (andylyg@umich.edu) and Zheng Chen (chen@kmust.edu.cn)

This work was funded in part by the National Science Foundation of China (No. U1764259), in part by Chongqing Fundamental Research and Frontier Exploration Project (No. CSTC2018JCYJAX0409), in part by the Fundamental Research Funds for the Central Universities (No. 2018CDJDCD0001 and 2018CDQYQC0035), and in part by the EU-funded Marie Skłodowska-Curie Individual Fellowships Project under Grant 845102-HOEMEV-H2020-MSCA-IF-2018.

ABSTRACT Identification of driving intentions has increasingly attracted wide attention since it can be a valuable reference input of vehicle intelligent control systems. In this study, the long short-term memory (LSTM) is employed to identify the longitudinal intention online with high precision. To this end, the driving intentions when the vehicle runs on a straight and flat road are divided into five categories. The vehicle driving states such as the vehicle speed and acceleration are pre-processed to label the road test data. Subsequently, a LSTM classification model is established to identify the driving intention with inputs of opening degree of the accelerator pedal, vehicle speed and brake pedal force. Identification results reveal that the highest accuracy of the proposed algorithm attains 95.36%, which is around 20% higher than that of the traditional back propagation neural network. Finally, a driving intention-perceptive gear shifting strategy is developed with the help of the built recognition algorithm, and simulation results highlight that the strategy can effectively reduce the number of shifts and achieve better fuel economy.

INDEX TERMS Driving intention, long short-term memory (LSTM), back propagation neural network (BPNN), dual clutch transmission (DCT), shift strategy, fuel economy.

I. INTRODUCTION

With the development of modern automobile technologies, research on driving intention identification has attracted wide attention, and full consideration of driving intentions can help optimize control of the vehicle powertrain, and improve transportation efficiency and traffic safety [1], [2]. In driving assistance systems, the driving intention identification technique can assist recognition of the driving pattern and provide the driver with early warning about the possible accidents [3], [4]. For the automatic transmission system of vehicles, effective driving intention identification can be beneficial to the development of advanced gear shifting strategies, which helps to improve the shifting efficiency and vehicle noise vibration and harshness (NVH) [5], [6].

Drivers need to take certain actions on the accelerator/braking pedal according to operating state of the vehicle, surrounding environment and driving habits, so as to attain the anticipated driving intention. Generally speaking, driving intentions can be classified into lateral intentions and longitudinal intentions depending on the control object. The lateral intentions mainly include the lane change, cornering, and straight driving with inputs of the yaw angle, steering wheel angle and steering wheel angular velocity [7]–[9]. On the other hand, the longitudinal intentions can be acceleration, deceleration and cruise with references of the opening degree of the acceleration pedal, its variation rate, and opening degree of the braking pedal together with its variation

The associate editor coordinating the review of this manuscript and approving it for publication was Rajeeb Dey.

rate [6], [10], [11]. Actually, driving intentions are difficult to be expressed by precise mathematical models, and accurate intention identification is a challenging task. Existing identification methods can be classified into three categories, i.e., fuzzy logic control [7], [12], hidden Markov models (HMMs) [13], [14], and neural networks (NNs) [15], [16].

Fuzzy logic control usually employs fuzzy logic tables to represent rules that characterize the driving intention. The fuzzy logic table is direct and easy to implement when identifying the driving intention. Reference [17] designs a fuzzy controller which adopts opening degree of the acceleration pedal and its variation rate as inputs and the acceleration intention as the output. On this account, the fuzzy logic rule table is constructed, and its effectiveness is verified. In [7], an adaptive fuzzy classification method is proposed to detect the lane change intention according to the gaze information, and the identification results highlight that the recognition accuracy of the left and right lane change is 89.3% and 86.3%, respectively. Although the result accuracy is relatively high, it is necessary to notice that the rulemaking of the fuzzy logic table is mostly achieved by experience or artificially. Moreover, it is difficult to set up an accurate criterion to evaluate the identification results.

As well known, hidden Markov models (HMMs) are widely used for analysis of time series data. As driving actions are essentially a continuous process varying with time, no doubt, the HMM can be applied in driving intention recognition for advanced driving assistant systems (ADASs) and active safety systems. In [18], to improve recognition accuracy of the model, a hybrid model based on Gaussian mixture-HMM (GHMM) and generalized growing and pruning radial basis function neural network (GGAP-RBFNN) is proposed to identify the braking intention. In [19], two continuous HMMs are constructed to characterize the lane change and lane keeping intention, and a threshold-based classification method is introduced to identify the driving behavior of the target vehicle. Experimental results manifest that the lane change intention can be predicted 4 seconds ahead of action. For estimating the intention at a road intersection, two algorithms based on the hybrid state framework are proposed: one is the HMM optimized by genetic algorithm (GA), and the other one is the discrete HMM method. The results show that the accuracy of these two methods is 89.45% and 97%, respectively [20], [21]. Actually, it is challenging to identify some confusing intention as it considers only state sequences with the greatest log likelihood and ignores other state sequences. Moreover, it is imperative to know the transition probability among all the hidden states as well as the output probability between the hidden state and visible state in advance.

Neural networks (NNs) are capable of learning the nonlinear characteristics inside a control object which is difficult to model in a deterministic manner. As such, NNs have been introduced to identify driving intentions in some special circumstances [22], [23]. In [24], the driver's starting intentions are defined as three modes, i.e., slow start, normal start and fast start, and the statistical law of the accelerator opening is set as the input of the back propagation NN (BPNN). In [25], a BPNN model is developed to predict the lane change intention. Numerical results show that the accuracy of predicting the lane change 1.5 seconds ahead of time is 85.44%. Since the driving intention is a continuous process, traditional NNs usually cannot consider the time series information therein, and may result in unsatisfactory and even wrong identification result. Recurrent NN (RNN) can use its internal state to process sequences of inputs, and is therefore suitable for driving intention identification. In [9], a RNN based algorithm is proposed to predict early driving intention at intersections. In [26], a framework incorporating the RNN and graphical model is introduced to predict the future lane change manipulation of neighboring vehicles. Nonetheless, traditional RNNs cannot deal with information with infinite distances due to the disadvantage of gradient explosion.

Identification of driving intentions keeps challenging since it cannot be conducted directly during driving and is identified only according to the driver's operations and vehicle status. In addition, the operations that constitute the driving intention occur in a specific chronological order. In essence, a major drawback of existing driving intention studies is that they are usually subjected to influence of human factors and do not consider the sequence information during driving. To overcome this defect, the long short-term memory (LSTM) algorithm is adopted to identify the driving intentions. LSTM is an improved RNN without any influences from human factors. By adding a forgotten gate in each hidden layer to remember long term information, the LSTM can avoid gradient explosion of the traditional RNN [27]–[29]. Traditional many-to-one architecture of LSTM takes a time-series window of feature vectors as input and outputs a classification vector in the last time step of the time-series window. In contrast, the sequence-to-sequence LSTM is capable of holistically exploiting the inherent dependency and correlation between the different sensor data captured at each time step of real driving cycle segments [15]. Motivated by this, in this study, the sequence-to-sequence LSTM network is introduced to train the model with a variety of offline data and then applied to identify the driving intention. To this end, the training data is collected by the real vehicle test, which is marked by acceleration, rapid acceleration, cruise, deceleration and rapid deceleration through a series of data preprocessing operation. The opening degree of the accelerator pedal, vehicle speed and brake pedal force are selected as characteristic parameters when training the LSTM model. The remaining data are used to verify the accuracy of model training. Numerical analysis results highlight the rationality of the proposed LSTM algorithm. Additionally, to validate applicability of the driving intention recognized by the built algorithm, the identification results are implemented to assist in developing a gear shift strategy. The simulation results show that the gear shifting strategy incorporating the proposed identification algorithm can conduct the shift gear more reasonably and thus lead to better fuel economy,

compared with that with the BPNN based identification algorithm.

The main contribution of this study can be attributed to the following two aspects: 1) the driving intention recognition problem is defined as a time series classification problem, and the intention of each step is identified by a sequence-to-sequence LSTM classification model; and 2) the recognition result of the driving intention is merged to facilitate the gear shifting control. The results manifest that the comprehensive shift strategy considering the LSTM recognition technique lead to fewer shift actions and better fuel economy.

The remainder of the paper is structured as follows. In Section II, the identification of the driving intention is expressed as a time series classification problem, and the structure of driving intention identification based on the LSTM is proposed. The data-preprocessing algorithm is introduced, and the LSTM model is established in Section III. In Section IV, the simulation analysis is conducted, and the recognition result based on LSTM is evaluated and compared with that of BPNN. In addition, a comprehensive shifting strategy based on the driving intention recognition result is discussed in Section V. Section VI draws the main conclusion of this study.

II. DRIVING INTENTION PROBLEM FORMULATION

The driver realizes his/her driving intention by manipulating the accelerator pedal or brake pedal according to the road condition and state of the vehicle. Consequently, the driving intention can be identified by analyzing the acceleration and braking pressure with combination of partial state parameters of the vehicle. This study focuses on the driving intention in the straight and flat road conditions, and the whole intention is divided into five discrete categories, i.e., acceleration, rapid acceleration, deceleration, rapid deceleration, and cruise, as listed in Table 1. Usually, the driving intention can be expressed as a nonlinear function related to the vehicle speed, accelerator pedal opening and brake pedal force:

$$I(t) = f(v(t), \alpha(t), b(t)) \tag{1}$$

where $I(t)$ expresses the driving intention, $v(t)$ is the vehicle speed, $\alpha(t)$ indicates the accelerator pedal opening degree, and $b(t)$ is the brake pedal force at time t.

As discussed before, the driving information collected by the sensor is essentially time series data and the simple mapping formulated in (1) does not take into account the relationship among time series samples, leading to instability of the driving intention identification. To further consider the time-varying characteristics, the identification of driving intentions issue can be updated, as:

$$I(1, 2, \cdots, t) = f(x(1), x(2), \cdots, x(t)) \tag{2}$$

where $x(t)$ is the sample vector at time t, and equals:

$$x(t) = \begin{bmatrix} v(t) \\ \alpha(t) \\ b(t) \end{bmatrix} \tag{3}$$

TABLE 1. Classification of driving intentions.

Intention class	Intention name
1	Acceleration
2	Rapid Acceleration
3	Cruise
4	Deceleration
5	Rapid Deceleration

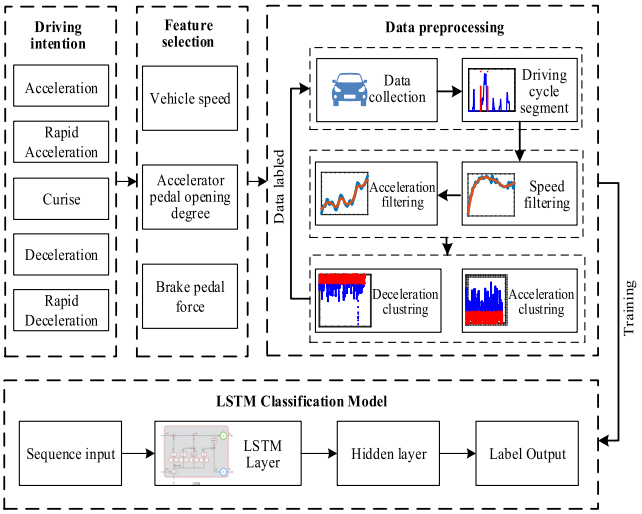

FIGURE 1. Structure of a driving intention identification model.

Actually, the essence of identifying the driving intention is determination of the intention category. It is a typical time series pattern recognition problem correlating to the driver's subjective expectation.

The whole identification framework is shown in Fig. 1, which shows that after determining the driving intention types and feature variables, the data preprocessing is conducted including the data collection, speed filtering and clustering analysis. On this basis, the LSTM model is built and finally, the driving intention is identified.

III. ESTABLISHMENT OF DRIVING INTENTION IDENTIFICATION MODEL BASED ON LSTM

A. DATA PREPROCESSING

A vehicle equipped with a 7-speed DCT is tested to acquire the driving data on a straight road. To simplify the problem, this study focuses on investigation of the driving intention on a flat road. The collected data mainly includes the vehicle speed, opening degree of the accelerator pedal and brake pedal force. These data are preprocessed with three main steps to form a database before accessing to the LSTM model:

1) DIVISION OF DRIVING CYCLE SEGMENT

To eliminate impact of the data value of zero caused by frequent stop on the model training, the data segment with the velocity of zero is removed. The driving process of each

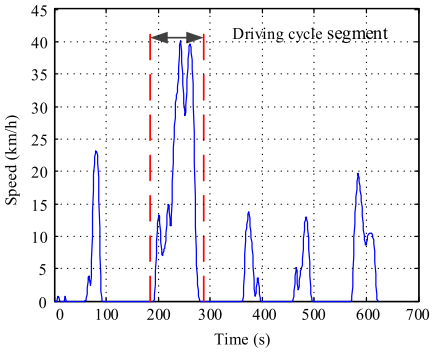

FIGURE 2. Division of driving cycle segment.

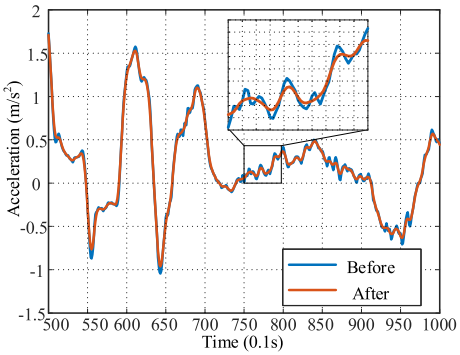

FIGURE 3. The filtering results of the vehicle acceleration.

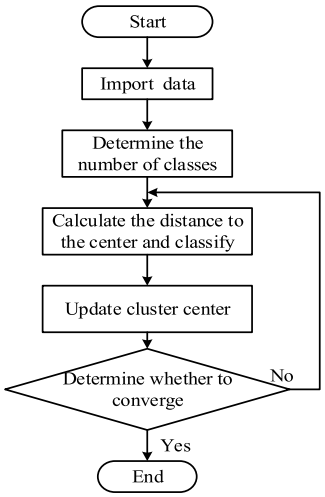

FIGURE 4. Flowchart of K-means clustering algorithm.

test driver is divided into multiple segments, and each section takes the speed of zero as the starting and ending point, as shown in Fig. 2. The sampling frequency is 10 Hz, and the whole testing cycle is divided into 130 segments in total, each of which includes 300 to 5000 sampling points.

2) ACCELERATION PROCESSING

The acceleration of the vehicle can be calculated according to derivation of the vehicle speed. However, direct derivation of the vehicle velocity often generates certain noise of the acceleration. By considering influences of sensor accuracy and road condition on the vehicle speed and acceleration, we employ the local weighted regression scatter smoothing (LOWESS) filter to smooth the acceleration signal.

The LOWESS algorithm is a commonly smoothing filter, of which the main idea is to take a point p as the center and intercept a piece of data with the length of f_{rac} forward and backward. For each piece of data segment, the weight function w is leveraged to conduct a weighted linear regression. For all n sampling points, n weighted regression lines can be generated, and the line connecting the center values of each regression line expresses the LOWESS curve of this data. The data length f_{rac} selected in this paper is 10, and the weight function w is a cubic function, as:

$$w(p) = \begin{cases} (1-p^3)^3, & for\ |p| < 1 \\ 0, & for\ |p| \geq 1 \end{cases} \tag{4}$$

where p represents the sampling points that need to be filtered. In this paper, it refers to the speed and derivation of the vehicle speed.

The smoothing results of the vehicle acceleration is described in Fig. 3. As can be seen, the filtered acceleration curve is close to the original data and smoother than before.

3) DETERMINATION OF THE THRESHOLD OF RAPID DRIVING OPERATION AND NORMAL DRIVING OPERATION

The driver's manipulation is directly expressed by the opening degree of the accelerating pedal and braking pedal, and the steering wheel angle. The longitudinal acceleration of the vehicle can fully reflect the driving intention on a straight line. Based on the vehicle longitudinal dynamics model, when the acceleration is zero and the velocity is not zero, we define now the vehicle is under the cruise state. However, during the actual driving process, due to unevenness of the road surface and sensitivity of the throttle opening degree, the driver may have a certain range of fluctuation in the cruise. For ease of handling it, the interval where the vehicle speed of greater than 20 km/h and the absolute acceleration of less than 0.2 m/s^2 is defined as the cruise action. The rapid and normal acceleration / deceleration threshold values are decided by means of the K-means algorithm.

The K-means algorithm is widely applied which features fast convergence and simple calculation. The K-means algorithm is an unsupervised learning method, and its calculation flowchart is illustrated in Fig. 4. First, a category number k (k >0) is given, then the distance between each sample and the clustering center is calculated, and the sample to the nearest cluster center is assigned. Next, the cluster center and sample category are continuously adjusted, and all the data are finally divided into k categories, which satisfy the principle of high similarity between the same category and least similarity among different classes. The similarity is herein defined by the Euclidean distance, which is expressed as:

$$d_{xy} = \sqrt{\sum_{i=1}^{n} (x_i - y_i)^2} \tag{5}$$

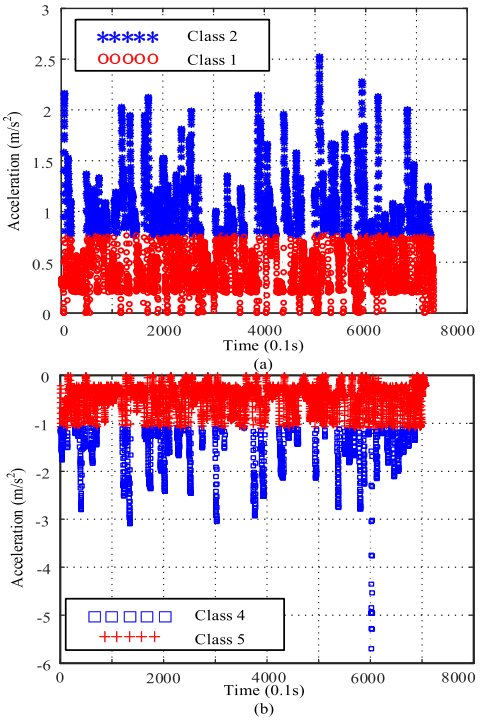

FIGURE 5. (a) Threshold of acceleration and rapid acceleration; and (b) threshold of deceleration and rapid deceleration.

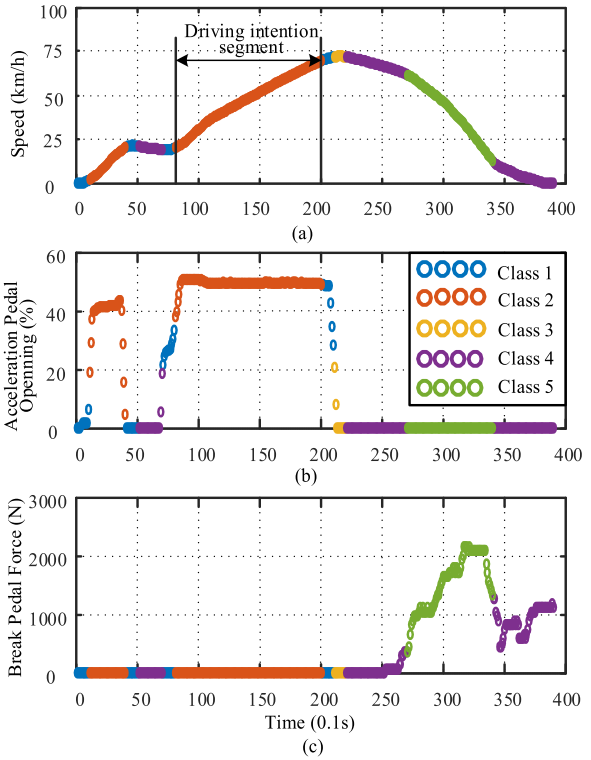

FIGURE 6. Labeled Data. (a) Speed; (b) opening degree of the acceleration pedal; and (c) braking pedal force.

where x denotes the sampling data of acceleration, y expresses the cluster center, and n represents the number of characteristic parameters of the clustering center. In this paper, since the goal of clustering is to distinguish the rapid operation from the normal action, the acceleration is selected as the feature of the cluster and n equals 1.

The threshold of acceleration and rapid acceleration as well as deceleration and rapid deceleration are determined according to the K-means clustering algorithm, as shown in Fig. 5. As can be found, the threshold of acceleration and rapid acceleration is set to 0.7 m/s^2, and the threshold of deceleration and rapid deceleration is imposed to be -1.1 m/s^2. Through the clustering of acceleration, the vehicle speed, accelerator pedal opening and brake pedal force collected by the actual vehicle is labeled, shown in Fig. 6, and different color denotes different intention. As can be seen, during 0 to 40 s, the driving intention belongs to acceleration and rapid acceleration. In this stage, the throttle opening degree gradually increases, and the brake pedal force is always zero.

Similar to the definition of the driving cycle segment, the driving intention segment is defined from the beginning to the end of a certain interval, as shown in Fig. 6 (a). The number of driving intention segments included in the marked 130 cycle segments is shown in Table 2. We can find that the acceleration intention sections appear most frequently during driving with a total number of 1848. The number of cruise and deceleration sections is almost the same. In addition, the numbers of rapid acceleration and rapid deceleration sections are relatively smaller, which is 656 and 557, respectively.

TABLE 2. Number of intention segment.

Intention class	Intention name	Amount
1	Acceleration	1848
2	Rapid Acceleration	656
3	Cruise	1719
4	Deceleration	1622
5	Rapid Deceleration	557

In summary, the driving intention segments marked includes all possible situations and is suitable for training of the LSTM model.

B. ESTABLISHMENT OF THE LSTM CLASSIFICATION MODEL

The structure of a sequence-to-sequence LSTM for classification consists of the input layer, LSTM layer, fully connected (FC) layer, softmax layer and classification output layer. It is necessary to mention that the LSTM layer consists of five parts: a cell unit c_t for storing the long-term state, a cell state $\tilde{c}_t$ for describing the current input, and three gates including a forget gate f_t, an input gate i_t and an output gate o_t. The gate is essentially a FC layer, of which the input is a vector and the output is a Boolean vector.

The sequence sample data after preprocessing and its corresponding categories are the input and the desired output of the LSTM classification model which can be expressed as:

$$\begin{cases} x^{(m)} = (x_1, x_2, x_3, \cdots, x_N) \\ I^{(m)} \in \{1, 2, 3, 4, 5\} \end{cases} \tag{6}$$

where $x^{(m)}$ denotes the time series sample of the mth segment, x_N expresses the sample vector at step N, and $I^{(m)}$ represents the category of $x^{(m)}$.

The data on the structure are transmitted between layers by regulating the weight vectors, bias terms and transfer function of the neurons within each layer. Therefore, determination of the weights, biases and transfer functions becomes the key procedure for training the algorithm. Assuming that the sample vector at time t is x_t, the steps for training the LSTM model can be detailed as follows:

1) Load the time series sample vector x_t:

$$x_t = \begin{bmatrix} v(t) \\ \alpha(t) \\ b(t) \end{bmatrix} \tag{7}$$

2) Determine the information of cell states that needs to be abandoned. By supposing that the input of this step is x_t and the output of the previous LSTM layer is h_{t-1}, the output f_t can be expressed as:

$$f_t = \sigma(w_f[h_{t-1}, x_t] + b_f) \tag{8}$$

where w_f and b_f denote the weight vector and the bias term of forget gate f_t; and σ is the sigmoid function.

3) Select what information needs to be stored in the new cell unit c_t. First, the sigmoid layer i_t decides which values needs to be updated. Then, the tanh layer creates a vector $\tilde{c}_t$ of new candidate values. Next, these two procedures are combined to update the old cell unit c_{t-1} to a new cell unit c_t, as:

$$\begin{cases} i_t = \sigma(w_i \cdot [h_{t-1}, x_t] + b_i) \\ \tilde{c}_t = \tanh(w_c \cdot [h_{t-1}, x_t] + b_c) \\ c_t = f_t \cdot c_{t-1} + i_t \cdot \tilde{c}_t \end{cases} \tag{9}$$

where w_i and w_c denote the weight vector of input gate i_t and cell unit of the current time $\tilde{c}_t$, respectively; and b_i and b_c express the bias of the corresponding gate.

4) Update the hidden state h_t and calculate the output gate o_t:

$$\begin{cases} o_t = \sigma(w_o \cdot [h_{t-1}, x_t] + b_o) \\ h_t = o_t \cdot \tanh(c_t) \end{cases} \tag{10}$$

where w_o and b_o denote the weight vector and bias term of output gate o_t, respectively. Actually, steps 2) to 4) constitute the training process of the LSTM layer, and Fig. 7 shows the flowchart of time series data with three driving feature quantities trained in the LSTM layer [30].

5) Transmit the output of the LSTM layer to the FC layer. The main purpose is to convert the previous output into the identified intention, and the output is the score of each category z_j, as:

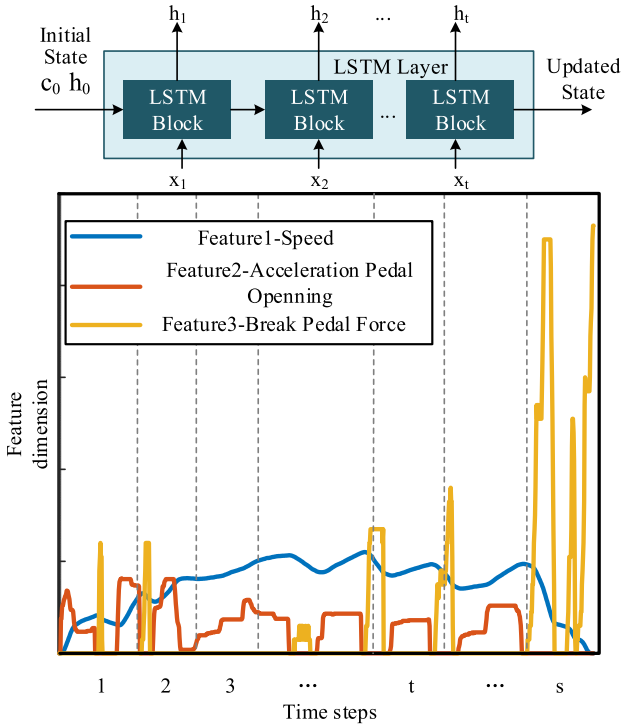

FIGURE 7. Flow of time series data in the LSTM layer.

$$z_j = w_j \cdot x(t) + b_j \tag{11}$$

where w_j and b_j denote the weight vector and bias of category j, respectively. Since the driving intentions are divided into five categories, the size of the full connection layer is five.

6) Take the output of the FC layer as input and determine the probability of each category on all possible target classes, we can get:

$$\hat{y}_j = softmax(z_j) = \frac{e^{z_j}}{\sum_{j=1}^{c} e^{z_j}} \tag{12}$$

where z_j is score of category j, and c is the number of categories and equals 5 in this study.

7) Finally, achieve the recognition and obtain the identification result I_t with highest probability.

Since the adaptive moment estimation (ADAM) is a first-order optimization algorithm that iteratively updates neural network weights based on the training data [31], it is consequently herein introduced to specify an initial learning rate of 0.01, and then the learning rate was lowered by a default factor of 0.1 after 20 periods. To prevent gradient explosion, we set the gradient threshold to 1. Subsequently, the gradient decay factor and squared gradient decay factor are set to 0.9 and 0.999, respectively. When training the LSTM model, all the above setting process is repeated, and all the weight vectors and bias terms need to be updated periodically.

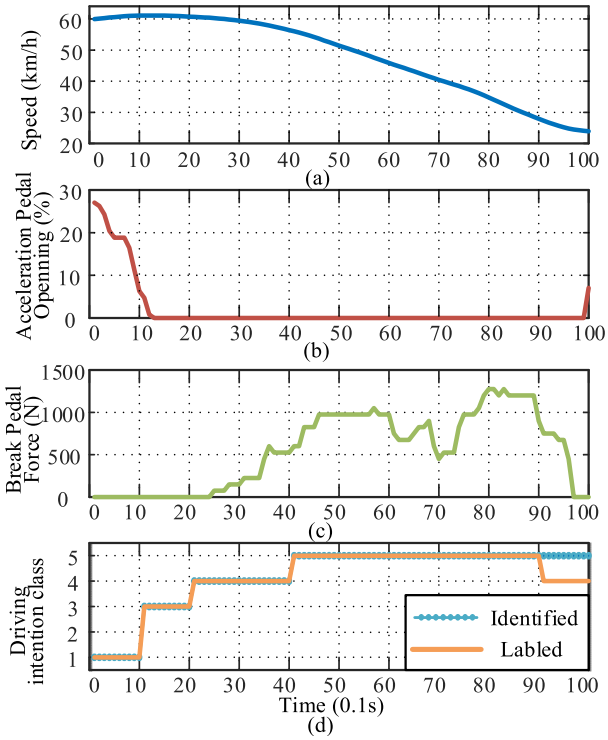

FIGURE 8. (a) Speed; (b) acceleration pedal opening; (c) brake pedal force; and (d) recognition result of driving intention.

IV. SIMULATION AND ANALYSIS

The simulation validation is divided into two parts. First, the effectiveness of the LSTM based driving intention recognition model is analyzed. Then, the driving intention recognition result of the LSTM model is compared with that of the BPNN model.

A. ANALYSIS OF EFFECTIVENESS OF DRIVING INTENTION RECOGNITION MODEL BASED ON LSTM

In this paper, 116 driving cycle segments are used for training the model and the remaining 14 segments are implemented to validate the LSTM model. The driving intention is identified with a time step of 0.1 s and the time window is chosen to be 1 s. Thus, the main intention of these 10 steps represents that of the entire sequence. Here, we employ the majority voting method, rather than the prediction result of each time step, to determine the sequence intention, and meanwhile to avoid the influence induced by the prediction error of each interval. The recognition result is shown in Fig. 8.

Figs. 8 (a), (b) and (c) show the speed, opening degree of the accelerator pedal and brake pedal force within 100 sampling points of a certain segment. It can be found that the opening degree of the accelerator pedal decreases from 30% to 0 in 2 s, and the brake pedal force is always 0 in this period; after 2 s, the throttle opening degree is 0, and the brake pedal force gradually increases. As can be seen in Fig. 8 (d), the driving intention recognition result changes from acceleration to cruise after 2 s. Then, it keeps deceleration during 2 to 4 s. In the following, the intention becomes rapid deceleration after 4 s. However, in the last second, the deceleration is mistakenly recognized as a rapid deceleration.

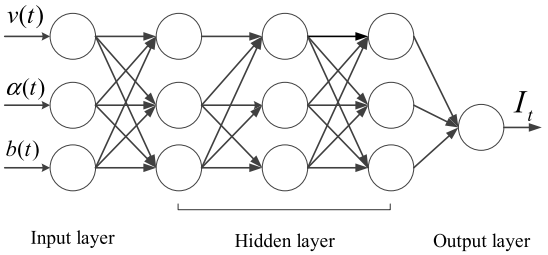

FIGURE 9. Structural sketch of the BPNN.

B. COMPARISON OF RECOGNITION RESULTS

To evaluate the performance of the proposed method, the confusion matrix of each class is selected, and the overall accuracy and precision are employed as evaluation indicators [32]. The confusion matrix is a popular manner to evaluate the performance of machine learning algorithms. It is a square matrix, whose dimension equals the category numbers [33]. For $i, j \in \{1, \ldots, N_c\}$, supposing that M_{ij} and C_j represent the element of confusion matrix and sample set from the class j, and $h(I_k)$ expresses the identification output of the sample I_k, we can attain:

$$\begin{cases} M_{ij} = \left|\left\{I_k \in C_j : h(I_k) = i\right\}\right| \\ Accuracy = \sum_{j=1}^{Nc} M_{ij} / \sum_{j=1}^{Nc} \left|C_j\right| \\ Precision(i) = M_{ii} / \sum_{j=1}^{Nc} M_{ij} \end{cases} \tag{13}$$

To compare the performance of the proposed algorithm, the BPNN method is also introduced to conduct the driving intention identification. BPNN is a typical NN consisting of an input layer, a hidden layer and an output layer. The number of neurons in the input and output layer is the same as the dimension of the input and output data, and the structure is shown in Fig. 9. In this paper, the input data includes the accelerator pedal opening degree, brake pedal force, and vehicle speed; and the output is the driving intention.

Table 3 shows the confusion matrix of two algorithms for a specific driving segment. Confusion matrix is a standard format for the accuracy evaluation. In general, accuracy is an assessment of the overall correctness of the classifier, and precision is an evaluation of the correct rate for a certain category. The recognition accuracy and average precision of LSTM is 92.5% and 94.6%, while that of BPNN is only 80.4% and 83.1% as a contrast. It can be found that the acceleration intention is easily identified as the rapid acceleration by both algorithms, whereas a small part is identified as the cruise intention by the BPNN algorithm. A small portion of the rapid acceleration intention is identified as acceleration; and the cruise intention is easy to be recognized

TABLE 3. Confusion matrix.

Method		Intention labeled					P (%)	AP (%)	A (%)
		1	2	3	4	5			
LSTM	1	310	40	20	0	0	83.8	94.6	92.5
	2	10	190	0	0	0	95.0		
	3	0	0	150	0	0	100		
	4	0	0	10	159	0	94.1		
	5	0	0	0	0	180	100		
BPNN	1	210	30	0	0	0	87.5	83.1	80.4
	2	100	200	20	0	0	62.5		
	3	10	0	130	10	0	86.7		
	4	0	0	30	149	10	78.8		
	5	0	0	0	0	170	100		

Note: P, AP and A represents precision, average precision and accuracy, respectively.

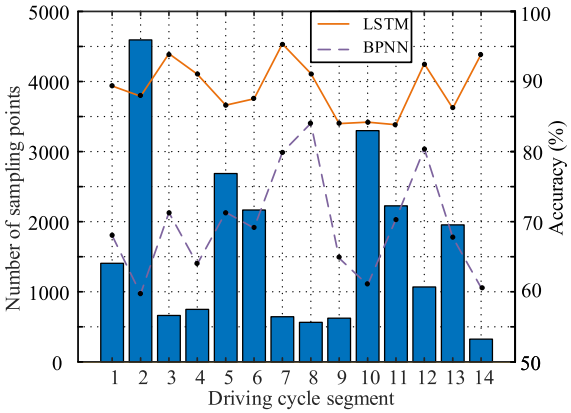

FIGURE 10. Accuracy of recognition results.

as acceleration and deceleration. In addition, some deceleration is misrecognized as cruise and the rapid deceleration intention is partly identified as the deceleration intention by the BPNN algorithm. It is necessary to mention that none of the deceleration and rapid deceleration is misidentified by the LSTM algorithm. In summary, we can find that the proposed LSTM method suggests higher precision in comparison with the BPNN.

The overall accuracy of the recognition result based on the two algorithms is compared in Fig. 10. It can be easily found that among the 14 driving cycle segments, the highest recognition accuracy of LSTM is 95.36%, and the number of sampling points is 646. Nonetheless, BPNN only shows the highest accuracy of 84.04% at the sampling point of 564. However, as can be calculated from Fig. 9, the overall average accuracy of the LSTM reached 89.11%, which is around 20% higher than that of the BPNN, verifying its feasibility.

In the next step, a case study in optimization of the gear shifting is investigated to extend application of the proposed identification algorithm.

V. A CASE STUDY IN OPTIMIZATION OF SHIFTING STRATEGY

Nowadays, more and more vehicles are equipped with dual clutch automatic transmissions (DCTs) to improve the transmission efficiency and fast shifting response, wherein the shifting strategies can show an important influence on vehicle dynamic performance and fuel economy. Many researches with respect to the shift schedule design and optimization have been widely investigated. In [34], an intelligent shifting strategy is proposed which is comprised of three schemes, i.e., the dynamic shifting strategy for uphill, safety scheme for downhill and economic rules for gentle slopes. In [35], the fuzzy decision of shifting time and model-based torque coordinating control strategy are simultaneously conducted in terms of different driving intention. In [36], the optimal gear shifting strategy of EVs is developed by solving a nonlinear time-varying optimal problem, wherein the equivalent energy consumption including motor power and travelling distance is chosen as the objective function.

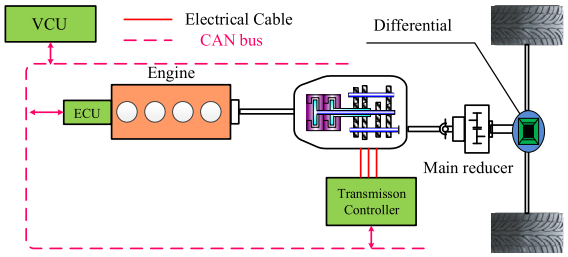

FIGURE 11. Schematic diagram of the vehicle.

Currently, most of commercial cars equipped with DCTs conduct the gear shifting by considering two typical parameters, i.e., the vehicle speed and throttle opening. However, these strategies require stable driving actions, and sudden change of the driver's intention and dramatic variation of the throttle opening may easily lead to frequent, accidental, circular, and undesired shift. It is imperative to devise a comprehensive shifting strategy incorporating the driver's intention, thereby tuning the DCT into the optimal gear according to the requirement and thus improving the vehicle's dynamic performance and fuel economy. However, the traditional two-parameter based strategy can be considered as the benchmark for evaluating control performance of the newly designed shifting strategy.

A. TRADITIONAL SHIFTING STRATEGY

To investigate the shifting strategy, a conventional engine-powered vehicle is simulated, shown in Fig. 11, and it mainly consists of an engine, a clutch as well a DCT. We applied an interpolation model to describe the nonlinear relationship among the engine fuel rate, engine torque, throttle opening and engine speed. The engine torque under different throttle opening and speed can be determined, as shown in Fig. 12 (a). In addition, the engine fuel rate with respect to different torque and speed is calibrated, as illustrated in Fig. 12 (b). By applying the interpolation-fitting algorithm, the engine torque and engine fuel consumption can be calculated. The basic parameters of the vehicle are listed in Table 4. Fig. 13 shows the traditional shifting strategy based on two typical parameters for the studied 7-speed DCT. Fig. 13 (a) describes

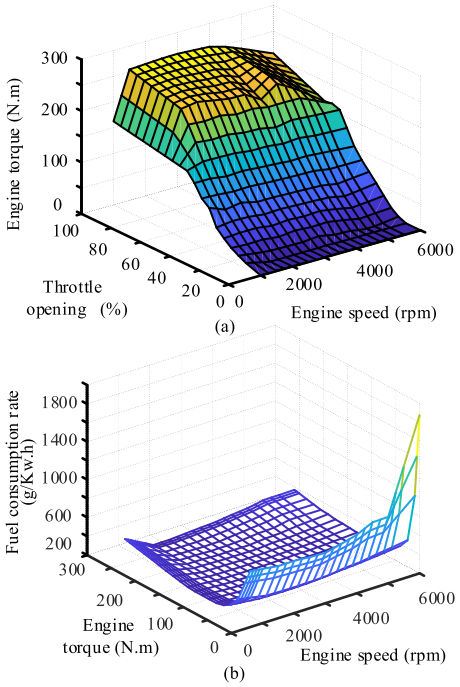

FIGURE 12. Engine map. (a) Engine torque map; and (b) engine fuel consumption map.

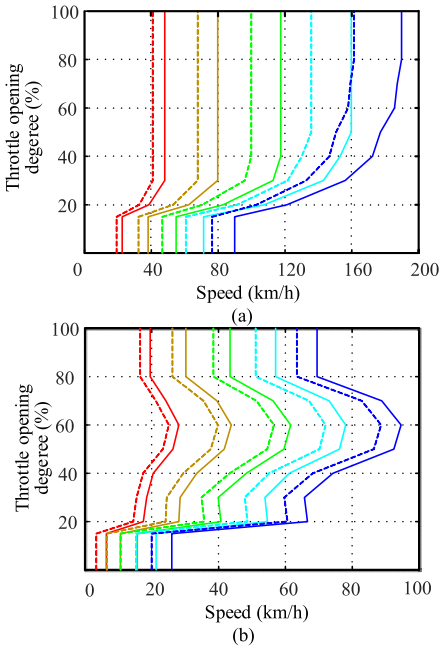

FIGURE 13. Shifting strategy. (a) For optimal power performance; and (b) for optimal fuel economy.

the strategy for optimal power performance, and Fig. 13 (b) shows the target of optimal fuel economy.

B. COMPREHENSIVE SHIFT STRATEGY BASED ON DRIVING INTENTION RECOGNITION RESULTS

After identifying the driving intention, the corresponding shifting strategy can be designed to verify the effect of driving

TABLE 4. Basic parameters of the vehicle.

Parameter	Value
Vehicle mass	1620 Kg (no load)/ 1995 Kg (full load)
Frontal area	2.6 m2
Wind resistance coefficient	0.36
Tire rolling radius	0.358 m
Transmission system efficiency	93%
Gear ratios	[4.214, 3.105, 1.724, 1.268, 1.27, 1.049, 0.891]
Main reducer gear ratio	[3.944, 3.227]

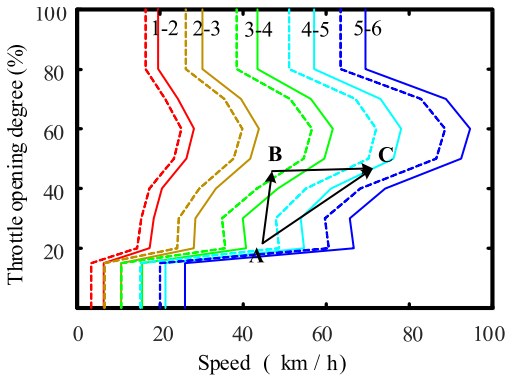

FIGURE 14. The shifting process when acceleration.

intention recognition in the gear shifting decision process. In normal acceleration stage, we adopt the shifting principle of targeting the preferable driving dynamics. However, it is imperative to note that since now the driving intention can be accurately identified, the properly delayed downshift can lead to unnecessary repetitive shifting action; and in this manner, the driving comfort can be ensured and meanwhile the fuel economy can be improved to a degree. Fig. 14 details the gear shifting process, and we can observe that the vehicle originally drives with the fourth gear and needs to change to the third gear once the acceleration is activated, as shown in the line AB. When the throttle opening is stable, the vehicle speed increases slowly and the gear ratio would cross the upshift line. As the line BC indicates, the vehicle is stepped into the fourth and fifth gear. As such, the vehicle shifts frequently with the price of loss of dynamic performance and comfort. On the other hand, when the engine speed and the throttle opening are determined, the fuel consumption is a certain value; however, the vehicle speed may be different due to different gear ratios. Certainly, lower gear may lead to lower vehicle speed, and the total fuel consumption with the lower gear in a fixed driving distance is more than that with the higher gear because of longer driving duration. In this context, if the algorithm can facilitate the delay of downshift in acceleration, the frequent shifting phenomenon can be avoided, and simultaneously the fuel consumption can be possibly reduced from this point of view. In addition, the optimal power performance and fuel economy should be traded off when designing the strategy [37].

TABLE 5. The value of the shift line correction factor.

Intention class	α_{up}	β_{up}	α_{down}	β_{down}
1-Acceleration	0.5	0.5	0.5	0.5
2-Rapid Acceleration	0	1	0	1
3-Cruise	1	1	0	0
4-Deceleration	1	1	0.5	0.5
5-Rapid Deceleration	1	1	0	1

Similarly, for the rapid acceleration, the shift strategy for the optimal power performance should be adopted as the predominant target. For the cruise process, the current driving state should be kept, and the gear position does not need to change. In terms of deceleration, the upshift should be avoided, and the downshift strategy should be balanced between the optimal power performance and fuel economy. With respect to the rapid deceleration, since the driver prefers stopping as soon as possible, the upshift should be prohibited and the main target of the downshift strategy should be the optimal power performance.

According to the identification result of driving intention, the comprehensive shift strategy is developed by interpolating between the shift line for the optimal power performance and fuel economy to adapt to different driving intentions. The correction can be formulated as:

$$\begin{cases} v_{up} = \alpha_{up} \cdot v_E^{up} + \beta_{up} \cdot v_P^{up} \\ v_{down} = \alpha_{down} \cdot v_E^{down} + \beta_{down} \cdot v_P^{down} \end{cases} \tag{14}$$

where v_{up} and v_{down} denote the modified upshift and downshift line, respectively; and v_E^{up}, v_E^{down}, v_P^{up} and v_P^{down} are upshift line and downshift line for optimal power performance and fuel economy, respectively. α_{up}, β_{up}, α_{down} and β_{down} express the correction factor of the upshift line and downshift line. Their detailed values are shown in Table 5.

C. SIMULATION ANALYSIS OF COMPREHENSIVE SHIFTING STRATEGY BASED ON RESULTS OF DRIVING INTENTION RECOGNITION

The studied vehicle is modeled, and a driving segment of around 400 s in the WLTC cycle is selected to validate the gear shifting performance. To achieve the target speed in the specific driving segment, the driver controller of the PID algorithm is introduced to regulate the vehicle speed and throttle opening degree. The main function of the driver model is to simulate his/her operation and control of opening degree of the accelerator pedal and braking pedal as well as the steering wheel angle. Since this study only considers the longitudinal motion of the vehicle, as shown in Fig. 15, the cycle velocity is regarded as the controlling target regulated by the PID controller. Since the parameters may show a great influence on the tracking precision, the three parameters of the controller are respectively set to 15, 12 and 0 after trail-and-error. The actual vehicle speed and accelerator opening degree of the driving cycle segment obtained by the driver

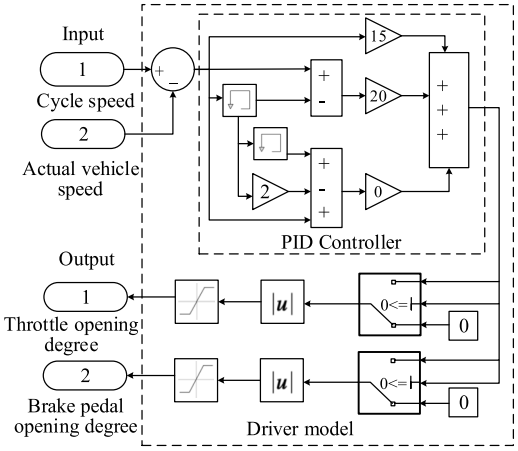

FIGURE 15. The driver model.

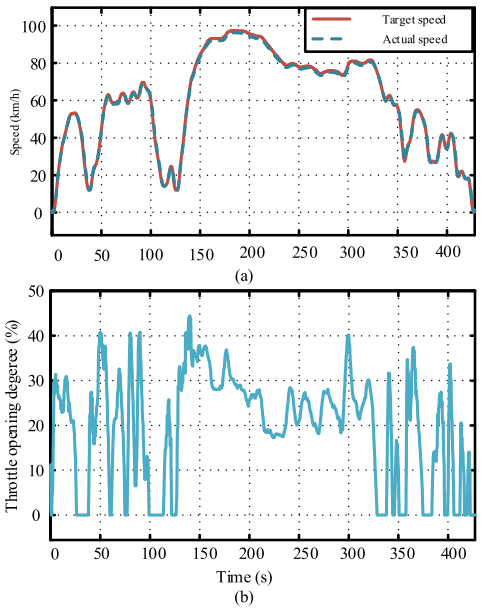

FIGURE 16. (a) Actual speed and target speed; and (b) throttle opening degree.

model is depicted in Fig. 16. As can be seen, the controller can enable the vehicle to track the target speed with satisfactory precision.

To analyze the influence of driving intention recognition results based on the comprehensive shift strategy, the recognition results of LSTM and BPNN are respectively employed for the gear shifting decision. The driving intention recognition process is shown in Fig. 17, and the simulated vehicle speed, accelerator opening and brake pedal force are sent to the trained LSTM model for the driving intention identification.

Fig. 18 shows the driving intention recognition results of proposed LSTM method and BPNN method for comparison. As can be seen, most of the recognition results of the two algorithms are the same. The selected WLTC cycle segment is simulated by the traditional shift strategies based on two

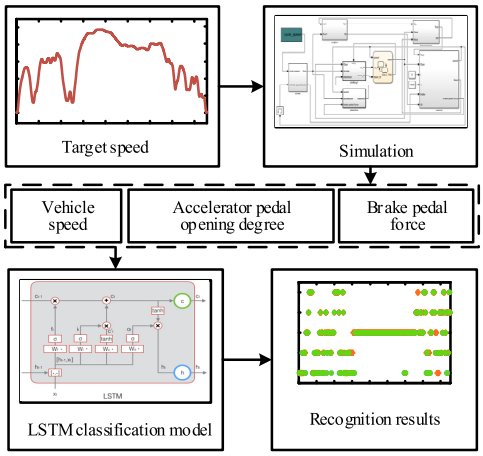

FIGURE 17. Process of driving intention identification.

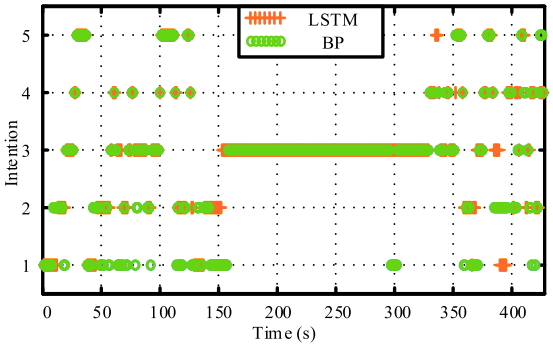

FIGURE 18. Driving intention recognition results of LSTM and BPNN.

typical parameters, as shown in Fig. 19 (a). The economic shift strategy is mainly to gain the optimal economic performance; by contrast, the dynamic shift strategy is to attain the optimal driving performance. As a result, with the same vehicle speed and accelerator pedal opening degree, the economic shift strategy tends to select a higher gear; however, the corresponding number of shifts can increase at the price of discounting the driving comfort.

Fig. 19 (b) shows the simulation results of the shift strategy based on LSTM and BPNN driving intention recognition results. During 0 to 40 s, the vehicle speed and the throttle opening gradually increases and then decreases, as shown in Fig. 16 (a). According to the economic shift strategy, the gearbox is gradually upgraded to the sixth gear and then lowered to the first gear. After considering the driving intention, the number of shifts is reduced. During 55 s to 105 s, the economic and dynamic strategy conducts shifts frequently among 2, 3 and 4 as well as 4, 5 and 6, respectively. The driving intention recognition result of LSTM is cruise and deceleration process at this stage. Since the comprehensive shifting strategy limits the upshift operation under the deceleration intention, the frequent shifting phenomenon is significantly reduced. Although BPNN recognizes the intention of cruise and deceleration, it also includes partial

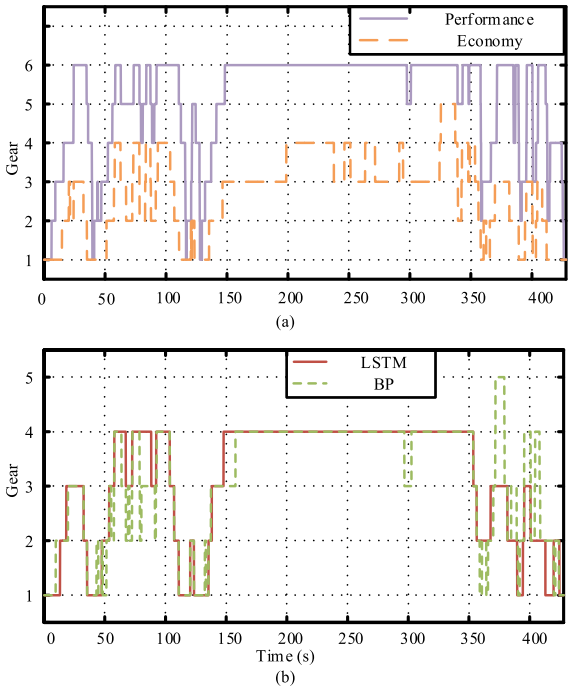

FIGURE 19. (a) Simulation results of traditional shift strategy; and (b) Simulation results of comprehensive shift strategy.

TABLE 6. Number of shifts and fuel consumption for different shift strategies.

Shift strategy		Number of shifts	Fuel consumption (ml)
Economy		86 (-)	464.7 (-22.9%)
Dynamic		64 (-25.6%)	602.7 (-)
Comprehensive	LSTM	30 (-65.1%)	504.8 (-16.2%)
	BP	64 (-25.6%)	525.2 (-12.9%)

Note: - : Reduction

recognition of acceleration, resulting in redundant upshift operations.

The engine fuel consumption is simulated, and the fuel consumption under the three shift strategies is compared in Table 6. It can be observed that after taking into account the driving intention, the shifting strategy can effectively reduce the number of shifts and achieve a better fuel economy simultaneously. By comparing the number of shifts based on the economy strategy, the comprehensive strategy can lead to a decrement of the shift number by 65.1% and 25.6%, respectively. Compared with the dynamic shifting strategy, the intention cognitive strategy can obviously reduce the fuel consumption. In summary, the proposed LTSM intention algorithm can be beneficial for improving the vehicle overall performance to a large extent. Therefore, the effectiveness of the proposed driving intention identification method applied in the shifting strategy is verified.

VI. CONCLUSION

This paper proposes a real-time driving intention identification method based on the LSTM network. Firstly, the driving intention identification problem is transformed into a time series classification issue. Then, the data collected by the vehicle test is marked by the K-means clustering method. Afterwards, the LSTM is applied to identify the driving intention with higher accuracy, in comparison with the traditional BPNN, thus verifying its feasibility. A comprehensive shifting strategy based on the driving intention recognition algorithm is developed. The simulation results manifest that the shifting strategy based on the LSTM recognition result can effectively reduce the number of shifts, and meanwhile significantly improve the fuel economy.

Next step work will focus on validation based on the hardware-in-the-loop platform and real vehicle test to further improve its real-time performance of the proposed algorithm.

REFERENCES

[1] C. Chen, L. Liu, T. Qiu, Z. Ren, J. Hu, and F. Ti, "Driver's intention identification and risk evaluation at intersections in the Internet of vehicles," *IEEE Internet Things J.*, vol. 5, no. 3, pp. 1575–1587, Jun. 2018.

[2] D. Yi, J. Su, C. Liu, and W.-H. Chen, "Trajectory clustering aided personalized driver intention prediction for intelligent vehicles," *IEEE Trans. Ind. Informat.*, vol. 15, no. 6, pp. 3693–3702, Jun. 2018.

[3] L. G. Hernández, O. M. Mozos, J. M. Ferrández, and J. M. Antelis, "EEG-based detection of braking intention under different car driving conditions," *Frontiers Neuroinform.*, vol. 12, p. 29, May 2018.

[4] M. Li, H. Cao, X. Song, Y. Huang, J. Wang, and Z. Huang, "Shared control driver assistance system based on driving intention and situation assessment," *IEEE Trans. Ind. Informat.*, vol. 14, no. 11, pp. 4982–4994, Nov. 2018.

[5] L. Li, X. Wang, R. Xiong, K. He, and X. Li, "AMT downshifting strategy design of HEV during regenerative braking process for energy conservation," *Appl. Energy*, vol. 183, no. 1, pp. 914–925, Dec. 2016.

[6] Y. Lei, Z. Yuanxia, Y. Fu, and K. Liu, "Research on adaptive gearshift decision method based on driving intention recognition," *Adv. Mech. Eng.*, vol. 10, no. 10, Oct. 2018, Art. no. 1687814018805353.

[7] F. Bocklisch, S. F. Bocklisch, M. Beggiato, and J. F. Krems, "Adaptive fuzzy pattern classification for the Online detection of driver lane change intention," *Neurocomputing*, vol. 262, pp. 148–158, Nov. 2017.

[8] K. Li, X. Wang, Y. Xu, and J. Wang, "Lane changing intention recognition based on speech recognition models," *Transp. Res. C, Emerg. Technol.*, vol. 69, pp. 497–514, Aug. 2016.

[9] A. Zyner, S. Worrall, and E. Nebot, "A recurrent neural network solution for predicting driver intention at unsignalized intersections," *IEEE Robot. Autom. Lett.*, vol. 3, no. 3, pp. 1759–1764, Jul. 2018.

[10] G. Qi, Y. Du, J. Wu, and M. Xu, "Leveraging longitudinal driving behaviour data with data mining techniques for driving style analysis," *IET Intell. Transp. Syst.*, vol. 9, no. 8, pp. 792–801, Oct. 2015.

[11] S. Fang, J. Song, H. Song, Y. Tai, F. Li, and T. S. Nguyen, "Design and control of a novel two-speed uninterrupted mechanical transmission for electric vehicles," *Mech. Syst. Signal Process.*, vol. 75, pp. 473–493, Jun. 2016.

[12] J. Heine, M. Sylla, I. Langer, T. Schramm, B. Abendroth, and R. Bruder, "Algorithm for driver intention detection with fuzzy logic and edit distance," in *Proc. IEEE 18th Int. Conf. Intell. Transp. Syst.*, Sep. 2015, pp. 1022–1027.

[13] S. Solaimanpour and P. Doshi, "A layered HMM for predicting motion of a leader in multi-robot settings," in *Proc. IEEE Int. Conf. Robot. Automat.*, May/Jun. 2017, pp. 788–793.

[14] D. Tran, W. Sheng, L. Li, and M. Liu, "A hidden Markov model based driver intention prediction system," in *Proc. IEEE Int. Conf. Cyber Technol. Automat., Control, Intell. Syst. (CYBER)*, Jun. 2015, pp. 115–120.

[15] K. Saleh, M. Hossny, and S. Nahavandi, "Driving behavior classification based on sensor data fusion using LSTM recurrent neural networks," in *Proc. IEEE Int. Conf. Intell. Transp. Syst.*, Oct. 2017, pp. 1–6.

[16] W. Shu, Y. Qiang, and Z. Xuan, "Study on driver's turning intention recognition hybrid model of GHMM and GGAP-RBF neural network," *Adv. Mech. Eng.*, vol. 10, no. 3, Mar. 2018, Art. no. 1687814018764985.

[17] B. Peng, H. Zhang, F. Xuan, and W. Xiao, "Torque distribution strategy of electric vehicle with in-wheel motors based on the identification of driving intention," *Automot. Innov.*, vol. 1, no. 2, pp. 140–146, Apr. 2018.

[18] X. Zhao, S. Wang, J. Ma, Q. Yu, Q. Gao, and M. Yu, "Identification of driver's braking intention based on a hybrid model of GHMM and GGAP-RBFNN," *Neural Comput. Appl.*, vol. 31, no. 1, pp. 161–174, Jan. 2019.

[19] Y. Zhang, Q. Lin, J. Wang, S. Verwer, and J. M. Dolan, "Lane-change intention estimation for car-following control in autonomous driving," *IEEE Trans. Intell. Veh.*, vol. 3, no. 3, pp. 276–286, Sep. 2018.

[20] S. B. Amsalu and A. Homaifar, "Driver behavior modeling near intersections using hidden Markov model based on genetic algorithm," in *Proc. IEEE Int. Conf. Intell. Transp. Eng.*, Aug. 2016, pp. 193–200.

[21] S. B. Amsalu, A. Homaifar, A. Karimoddini, and A. Kurt, "Driver intention estimation via discrete hidden Markov model," in *Proc. IEEE Int. Conf. Syst., Man, Cybern. (SMC)*, Oct. 2017, pp. 2712–2717.

[22] A. Díaz-Álvarez, M. Clavijo, F. Jiménez, E. Talavera, and F. Serradilla, "Modelling the human lane-change execution behaviour through multilayer perceptrons and convolutional neural networks," *Transp. Res. F, Traffic Psychol. Behav.*, vol. 56, pp. 134–148, Jul. 2018.

[23] X.-Y. Wang, Y-Q. Liu, Q. Xu, Y.-Y. Xia, H.-X. Zhao, S.-J. Liu, and J.-Y. Han, "Feature extraction and dynamic identification of driving intention adapting to multi-mode emotions," *Adv. Mech. Eng.*, vol. 11, no. 4, Apr. 2019, Art. no. 1687814019839906.

[24] L. Liang, Z. Zhu, X. Wang, Y. Yang, Y. Chao, and S. Jian, "Identification of a driver's starting intention based on an artificial neural network for vehicles equipped with an automated manual transmission," *Proc. Inst. Mech. Eng. D, J. Automobile Eng.*, vol. 230, no. 10, Oct. 2015, Art. no. 0954407015611294.

[25] J. Peng, Y. Guo, R. Fu, W. Yuan, and C. Wang, "Multi-parameter prediction of drivers' lane-changing behaviour with neural network model," *Appl. Ergonom.*, vol. 50, pp. 207–217, Sep. 2015.

[26] S. Patel, B. Griffin, K. Kusano, and J. J. Corso, "Predicting future lane changes of other highway vehicles using RNN-based deep models," Jan. 2018, *arXiv:1801.04340*. [Online]. Available: https://arxiv.org/abs/1801.04340

[27] P. Chantamit-O-Pas and M. Goyal, "Long short-term memory recurrent neural network for stroke prediction," in *Proc. Int. Conf. Mach. Learn. Data Mining Pattern Recognit.*, Jul. 2018, pp. 312–323.

[28] S. Petridis, Z. Li, and M. Pantic, "End-to-end visual speech recognition with LSTMS," in *Proc. IEEE Int. Conf. Acoustics, Speech Signal Process. (ICASSP)*, Mar. 2017, pp. 2592–2596.

[29] H. Sak, A. Senior, and F. Beaufays, "Long short-term memory recurrent neural network architectures for large scale acoustic modeling," in *Proc. 15th Annu. Conf. Int. Speech Commun. Assoc.*, Sep. 2014, pp. 338–342.

[30] K. Greff, R. K. Srivastava, J. Koutník, B. R. Steunebrink, and J. Schmidhuber, "LSTM: A search space odyssey," *IEEE Trans. Neural Netw. Learn. Syst.*, vol. 28, no. 10, pp. 2222–2232, Oct. 2017.

[31] D. P. Kingma and J. Ba. *Adam: A Method for Stochastic Optimization*. Accessed: Dec. 1, 2014. Available: https://ui.adsabs.harvard.edu/abs/2014arXiv1412.6980K

[32] L. Yang, R. Ma, H. M. Zhang, W. Guan, and S. Jiang, "Driving behavior recognition using EEG data from a simulated car-following experiment," *Accident Anal. Prevention*, vol. 116, pp. 30–40, Jul. 2018.

[33] N. Arbabzadeh and M. Jafari, "A data-driven approach for driving safety risk prediction using driver behavior and roadway information data," *IEEE Trans. Intell. Transp. Syst.*, vol. 19, no. 2, pp. 446–460, Feb. 2018.

[34] F. Meng and J. Hui, "Slope shift strategy for automatic transmission vehicles based on the road gradient," *Int. J. Automot. Technol.*, vol. 19, no. 3, pp. 509–521, Jun. 2018.

[35] Z. Zhao, H. Chen, and Y. Yang, "Fuzzy determination of target shifting time and torque control of shifting phase for dry dual clutch transmission," *Math. Problems Eng.*, vol. 2014, Feb. 2014. Art. no. 347490.

[36] L. Guo, B. Gao, and H. Chen, "Online shift schedule optimization of 2-speed electric vehicle using moving horizon strategy," *IEEE/ASME Trans. Mechatronics*, vol. 21, no. 6, pp. 2858–2869, Dec. 2016.

[37] W. Yang, Q. Chen, G. Wu, and D. Qin, "Design of the intelligent compensating shifting schedule and its application in dual clutch automatic transmission vehicle," *J. Mech. Eng.*, vol. 45, no. 1, pp. 205–210, 2009.

YONGGANG LIU received the B.S. and Ph.D. degrees in automotive engineering from Chongqing University, Chongqing, China, in 2004 and 2010, respectively.

He was a joint Ph.D. Student and a Research Scholar with the University of Michigan–Dearborn, MI, USA, from 2007 to 2009. He is currently a Professor and Dean Assistant with the School of Automotive Engineering, Chongqing University. He is also a Committee Member of the Vehicle Control and Intelligence Society of the Chinese Association of Automation (CAA). His research interests mainly include optimization and control of intelligent electric and hybrid vehicles and integrated control of vehicle automatic transmission systems. He has led more than ten research projects and published more than 50 research journal articles.

PAN ZHAO received the B.S. degree in mechanical engineering from the Hebei University of Technology, Tianjin, China, in 2017. She is currently pursuing the M.S. degree in mechanical engineering with Chongqing University, Chongqing, China.

Her research interests include intelligent control of dual clutch transmissions.

DATONG QIN received the B.S., M.S., and Ph.D. degrees in mechanical engineering from Chongqing University, Chongqing, China, in 1982, 1984, and 1993, respectively. In 1989, he was a joint Ph.D. student with Tohoku University, Sendai, Miyagi, Japan. He is currently a Professor with the State Key Laboratory of Mechanical Transmissions and the School of Automotive Engineering, Chongqing University. His research interests include control and application of mechanical transmission and vehicle power transmission. He has conducted more than 60 projects and has published more than 200 peer-reviewed journal articles and conference proceedings. He is the receiver of the Changjiang Scholars Program of China and two First Prizes of provincial-level scientific and technological progress awards, in 2008 and 2010.

GUANG LI received the Ph.D. degree in electrical and electronics engineering with a specialization in control systems from the University of Manchester, Manchester, U.K., in 2007.

He is currently a Senior Lecturer in dynamics modeling and control with the Queen Mary University of London, London, U.K. His research interests include constrained optimal control, model predictive control, adaptive robust control, and control applications, including renewable energies and energy storage.

ZHENG CHEN received the B.S. and M.S. degrees in electrical engineering and the Ph.D. degree in control science engineering from Northwestern Polytechnical University, Xi'an, China, in 2004, 2007, and 2012, respectively.

He is currently a Professor with the Faculty of Transportation Engineering, Kunming University of Science and Technology, Kunming, Yunnan, China. He was a Postdoctoral Fellow and a Research Scholar with the University of Michigan, Dearborn, MI, USA, from 2008 to 2014. His research interests include battery management systems, battery status estimation, and energy management of hybrid electric vehicles. He has conducted more than 20 projects and has published more than 80 peer-reviewed journal articles and conference proceedings. He is the receiver of the Yunnan Oversea High Talent Project, China, and received the second place of the IEEE VTS Motor Vehicles Challenge, in 2017 and 2018.

YI ZHANG received the B.S. degree in mechanical engineering from Central South University, Changsha, China, in 1982 and the M.S. and Ph.D. degrees in mechanical engineering from the University of Illinois, Chicago, USA, in 1985 and 1989, respectively.

He is currently a Professor with the Department of Mechanical Engineering, University of Michigan–Dearborn, USA. His research interests include design and analysis of gearing systems, theory of gearing and applications, vehicle powertrains, and design and analysis of power transmission systems. He has published dozens of academic articles in these areas. He has also published a book in automotive power transmission systems with John Wiley and Sons, in 2018.